DOSIMETRY OF SEVERAL DTPA RADIOPHARMACEUTICALS IN CISTERNOGRAPHY

Valerie A. Brookeman and Richard L. Morin

University of Florida College of Medicine and Veterans Administration Hospital, Gainesville, Florida

Previously published biologic distribution and clearance data for ^{169}Yb-DTPA in cisternography were utilized to obtain effective spinal segment clearance data for six other easily chelated radionuclides: ^{99m}Tc, ^{113m}In, ^{111}In, ^{67}Ga, ^{51}Cr, and ^{203}Pb. Absorbed radiation doses to the spinal cord and nerve roots were calculated for each radioactive DTPA compound, employing appropriate cylindrical geometry and reduction coefficients for the dose contributions from the electrons of each radionuclide. Doses are maximal at the surface and decrease rapidly with distance from the surface. The relative useful photon flux from each DTPA radiopharmaceutical for approximately the same average absorbed radiation dose to the spinal cord was determined. The results indicate that ^{111}In and ^{203}Pb should be considered as possible radionuclide tags for DTPA cisternographic imaging.

Radioactive diethylenetriamine pentaacetic acid (DTPA) offers several advantages over ^{131}I-IHSA for cisternography (*1–7*). We recently reported the distribution and clearance of ^{169}Yb-DTPA during cisternography and estimates of the absorbed radiation doses to the spinal cord and nerve roots (*7*).

In this report we present absorbed radiation doses to the spinal cord and nerve roots during cisternography for six other radionuclides that also may be chelated. The doses for ^{99m}Tc, ^{113m}In, ^{111}In, ^{67}Ga, ^{51}Cr, and ^{203}Pb (*1,2,5*) are calculated from the biologic distribution and clearance data obtained with ^{169}Yb-DTPA.

MATERIALS AND METHODS

Since the method of obtaining effective spinal activity clearance data, corrected for body background, has been fully described previously (*7*), it will only be summarized in this report. Following intrathecal administration of 1 mCi ^{169}Yb-DTPA, spinal counts were obtained using a scintillation camera and computer system, at the routine cisternographic imaging times of approximately 2, 6, 9, 24, and 48 hr after injection, from nine patients, all of whom exhibited delayed flow. No normals were present in the group. Utilizing appropriate ^{169}Yb counting standards, the net activity in each segment at each time was obtained for six equal spinal segments, about 1.75 in.

TABLE 1. EASILY CHELATED RADIONUCLIDES

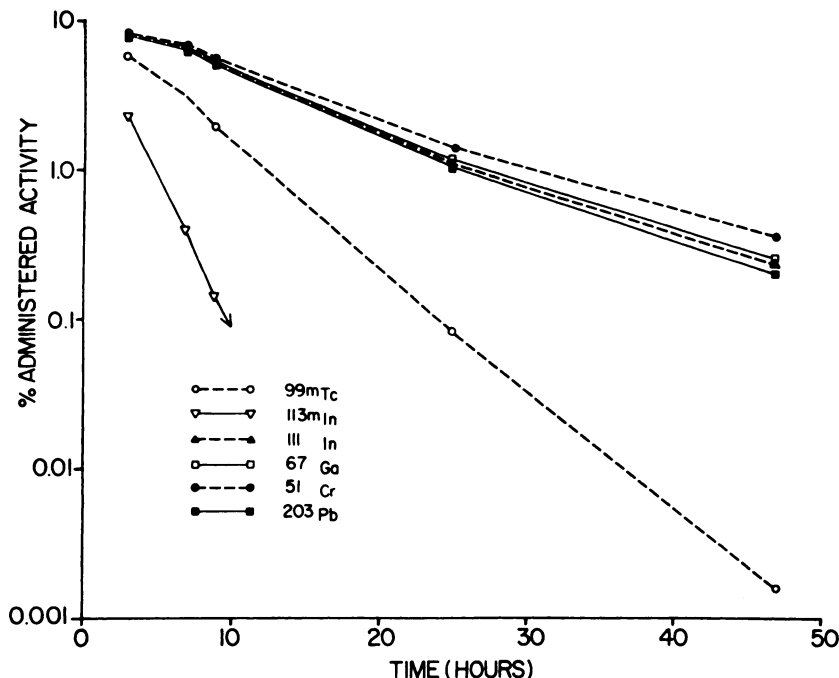| Radionuclide	Half-life (days)	Energies (keV)	Ranges in water (μm)	Net weighted mean energy (keV)	Range in water of mean energy (μm)
^{99m}Tc	0.25	0.4–142	0.02– 270	7	1.3
^{113m}In	0.07	0.7–392	0.04–1,230	98	130.0
^{111}In	2.81	0.6–246	0.03– 620	10	2.5
^{67}Ga	3.25	0.1–378	0.02–1,150	5	0.76
^{51}Cr	27.8	0.5–314	0.02– 890	2	0.14
^{203}Pb	2.17	3.0–666	0.33–2,560	21	9.0
^{169}Yb (7)	32.0	1.9–306	0.17– 830	13	5.0

FIG. 1. Mean activity–time curves for radioactive DTPA in spinal Segment 4 (cord).

wide by 5 in. long, numbered sequentially from 1 to 6 in the caudal direction from the base of the skull to the tip of the coccyx. Segments 1–4 contain the spinal cord and Segments 5 and 6 contain nerve roots. The injection site is in Segment 5. The calculated percentages of administered activity represented the activity remaining as a result of both physical decay and biologic clearance of ^{169}Yb-DTPA.

FIG. 2. Mean activity–time curves for radioactive DTPA in spinal Segment 5 (nerve roots).

The effective spinal segment clearance data for ^{169}Yb-DTPA (7) were converted to biologic clearance data by correcting for the physical decay of ^{169}Yb at each measurement time after injection. The biologic behavior of the DTPA chelate was assumed to be independent of the radionuclide tag (4,8,9). Hence, the resultant biologic clearance data were then corrected at each datum point for the physical decay of ^{99m}Tc, ^{113m}In, ^{111}In, ^{67}Ga, ^{51}Cr, and ^{203}Pb (Table 1) to yield effective spinal segment clearance data for each DTPA radiopharmaceutical.

RESULTS

Spinal segment activity. Curves of the mean percentage of administered activity for all patients as a function of time were derived for each spinal segment for each of the six DTPA radiopharmaceuticals. Figures 1 and 2 show these for spinal Segments 4 and 5 (the highest-activity segments containing spinal cord and nerve roots, respectively). All subsequent calculations and absorbed radiation dose estimates given for the spinal cord and nerve roots will be for spinal Segments 4 and 5.

Mean cumulated activities $\bar{A}$ were calculated for complete elimination of each DTPA radiopharmaceutical by graphic integration of the mean activity–time curves (Figs. 1 and 2), assuming, more conservatively, that elimination after the last datum point occurs solely by physical decay $\bar{A}(\infty)$ and, less conservatively, that the elimination rate obtained at the last datum point holds constant $\bar{A}(t_{eff})$ (7). Table 2 gives the cumulated activities for both elimination pathways for spinal cord and nerve roots for
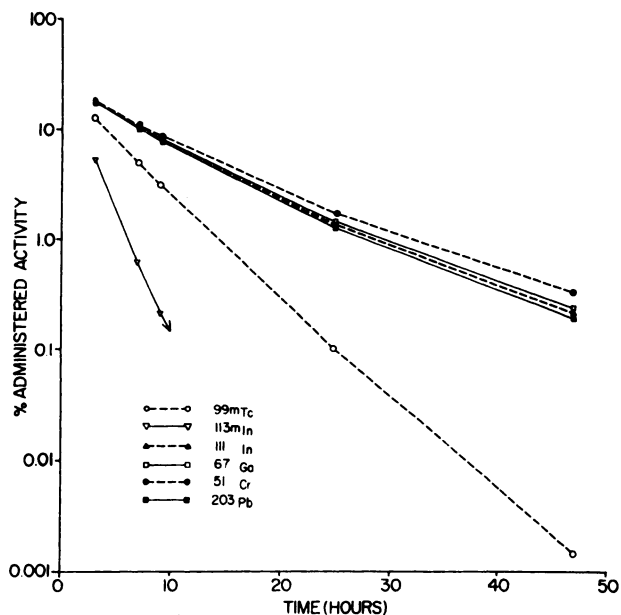
TABLE 2. ESTIMATED MEAN CUMULATED ACTIVITY AND PHOTON DOSE TO SPINAL CORD AND NERVE ROOTS FOR INTRATHECAL ADMINISTRATION OF 1 mCi RADIOACTIVE DTPA

Radionuclide	Spinal cord			Nerve roots		
	$\tilde{A}(\infty)$ (μCi-hr)	$\tilde{A}(t_{eff})$ (μCi-hr)	Mean $\bar{D}_{ph}$ (rad)	$\tilde{A}(\infty)$ (μCi-hr)	$\tilde{A}(t_{eff})$ (μCi-hr)	Mean $\bar{D}_{ph}$ (rad)
^{99m}Tc	585	585	0.2*	1,107	1,107	0.5*
^{113m}In	143	143	0.1*	303	303	0.4*
^{111}In	1,453	1,310	2.5 ± 0.1	2,378	2,241	4.9 ± 0.1
^{67}Ga	1,518	1,329	1.4 ± 0.1	2,451	2,270	2.8 ± 0.1
^{51}Cr	4,829	1,449	0.7 ± 0.4	5,655	2,437	1.0 ± 0.4
^{203}Pb	1,354	1,271	1.7 ± 0.1	2,263	2,184	3.5 ± 0.1
^{169}Yb (7)	5,376	1,457	5.3 ± 3.0	6,160	2,451	7.9 ± 3.4

* Range of doses < 0.05 rad.

intrathecal administration of 1 mCi of the six DTPA radiopharmaceuticals. Since both methods of determining cumulated activity are extreme cases, the values therefore represent minimum-to-maximum ranges.

Dosimetry. The general dose equation and reciprocity principle (10) were employed as described previously (7). The spinal fluid volumes used in determining absorbed dose estimates for the spinal cord (Segment 4) and nerve roots (Segment 5) were 18 and 15.5 ml, respectively (7). Published values of the equilibrium dose constant (Δ_i) were utilized for ^{99m}Tc, ^{113m}In, ^{51}Cr (11), and ^{67}Ga (12). The Δ_i values for ^{111}In and ^{203}Pb were obtained through the courtesy of Dr. Robert H. Rohrer (13). Tabulated values of the absorbed fraction ϕ_i(r ← v) for photons of energy 14-keV and above were utilized, assuming a uniformly distributed source in a small 20-gm ellipsoid surrounded by a scattering medium (14). For photons of energy less than 14 keV and greater than 7.5 keV, ϕ_i(r ← v) values were derived for a right circular cylinder of radius 0.8 cm and height 11.7 cm (7,15). Photons of energy 7.5 keV and less were assigned a ϕ_i(r ← v) value of 1. The values of $\Sigma_i \Delta_i \phi_i$(r ← v) for the photons of ^{99m}Tc, ^{113m}In, ^{111}In, ^{67}Ga, ^{51}Cr, and ^{203}Pb were 0.008, 0.018, 0.033, 0.018, 0.004, and 0.024 gm-rad/μCi-hr, respectively. The mean absorbed radiation doses from photons (D_{ph}) for 1 mCi of each DTPA radiopharmaceutical are given in Table 2 for the spinal cord and nerve roots.

The decay of each of the six radionuclides results in many low-energy internal-conversion and Auger electrons (Table 1), which are absorbed within very short distances from the surface of the spinal cord or nerve root. In order to determine accurately the mean absorbed radiation doses from electrons ($\bar{D}_e$) at different depths within the spinal cord and nerve roots, doses calculated from the
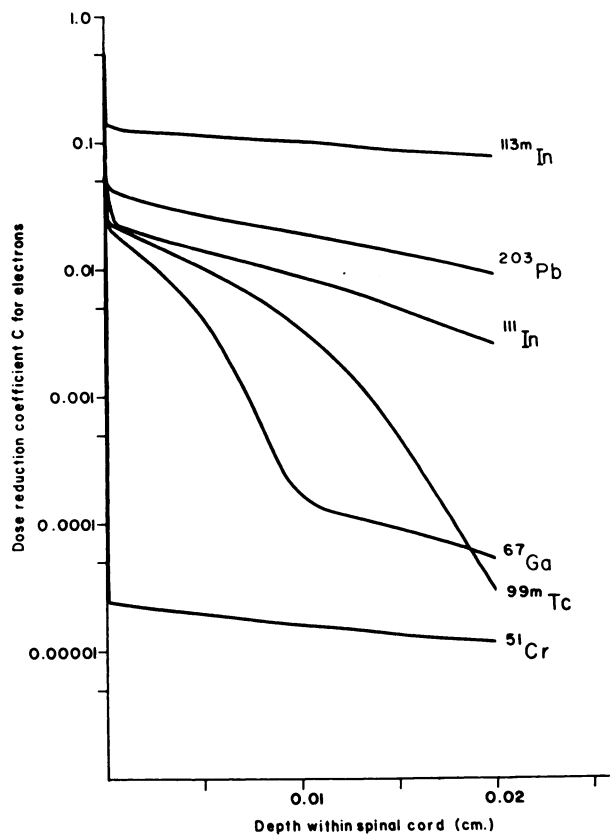
FIG. 3. Spinal cord dose reduction coefficients for electrons of six easily chelated radionuclides.

general dose equation (with $\phi_i = 1$) must be multiplied by a dose reduction coefficient C, which takes into account the presence of a cylindrical source-free region (the cord or nerve root) (7). Values of C were computed (16) for the six radionuclides from the data of Berger (17,18) for cylinders of radii r = 0.5 cm (cord) and r = 0.05 cm (nerve root) and are plotted in Figs. 3 and 4, respectively, as a function of the depth within the cord or nerve root from the surface. The C values are maximal at the sur-
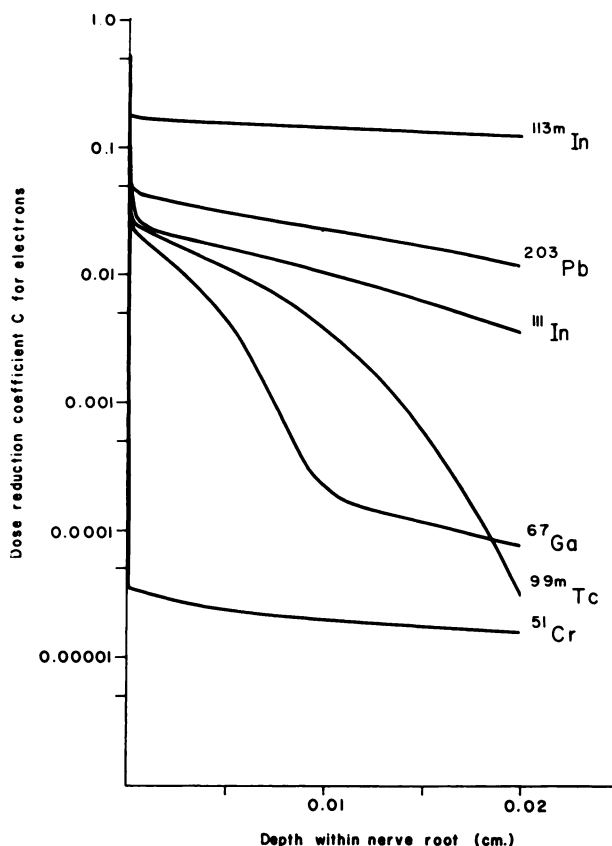
FIG. 4. Nerve root dose reduction coefficients for electrons of six easily chelated radionuclides.

at each depth for each radionuclide was applied to the electron contributions ($\overline{D}_e$) to the calculated mean absorbed doses. The total mean absorbed radiation doses ($\overline{D}_{ph} + \overline{D}_e$) per millicurie of each DTPA radiopharmaceutical at various depths from the surfaces of the cord and nerve roots are given in Table 3. Doses are maximal at the surface, where $\overline{D}_e$ ranges from 1.04$\overline{D}_{ph}$ for ^{51}Cr to 8$\overline{D}_{ph}$ for [113m]In. At 0.0001 cm, $\overline{D}_e$ is negligible compared to $\overline{D}_{ph}$ for ^{51}Cr-DTPA and less than 0.3$\overline{D}_{ph}$ for all the other radionuclides except [113m]In for which $\overline{D}_e$ is about 2.5$\overline{D}_{ph}$. By 0.01 cm, $\overline{D}_e$ is only 0.02$\overline{D}_{ph}$ or less for all the radionuclides except [203]Pb and [113m]In for which $\overline{D}_e$ is about 0.1$\overline{D}_{ph}$ and 2$\overline{D}_{ph}$, respectively.

DISCUSSION

The ranges given for the dose estimates in Tables 2 and 3 reflect the two methods of extrapolating the clearance data (Figs. 1 and 2) to infinity. There is, however, additional uncertainty in the dose estimates for the nerve roots due to the uncertainty of ±7.5 ml in the spinal fluid volume of 15.5 ml assigned to Segment 5 (7). Hence, all the dose estimates for the nerve roots may be additionally higher or lower by a factor of 1.9 or 0.7, respectively.

Since all patient data utilized in these absorbed radiation dose calculations showed slow cisternographic clearance (7), the cumulated activities and hence the dose estimates are higher than would be expected for cisternography in the normal individual.

Since the quoted thickness of the pia [0.01 cm (19)] only gives one order of magnitude, no precise delineation is made between "pia dose" and "cord dose." Hence the spinal cord doses in Table 3 are presented as a function of total depth from the surface including the thickness of the pia.

The absorbed radiation doses in Table 3 decrease rapidly with distance from the cord and nerve root surfaces and for all the radionuclide tags except [113m]In, reach their average values by 0.02 cm depth.

face and decrease very rapidly with distance from the surface. At 0.01 cm [the thickness of the pia (19)] from the surface of the cord or nerve root, absorbed radiation doses from electrons range from 0.004% of the surface doses for ^{51}Cr to 26% for [113m]In.

The values of $\Sigma_1 \Delta_i \phi_i (r \leftarrow v)$ for the electrons of ^{99m}Tc, [113m]In, ^{111}In, ^{67}Ga, ^{51}Cr, and [203]Pb were 0.036, 0.277, 0.077, 0.069, 0.008, and 0.116 gm-rad/μCi-hr, respectively. The appropriate value of C

TABLE 3. MEAN TOTAL ABSORBED DOSES (RADS) TO SPINAL CORD AND NERVE ROOTS PER MILLICURIE OF INTRATHECALLY ADMINISTERED RADIOACTIVE DTPA

Radio-nuclide	Depth within spinal cord from surface (cm)					Depth within nerve root from surface (cm)				
	0.0	0.0001	0.001	0.01	0.02	0.0	0.0001	0.001	0.01	0.02
[99m]Tc*	0.8	0.3	0.3	0.2	0.2	1.8	0.6	0.6	0.5	0.5
[113m]In*	1.2	0.4	0.4	0.4	0.3	3.3	1.3	1.2	1.1	1.0
[111]In	5.3 ± 0.3	2.7 ± 0.2	2.6 ± 0.1	2.5 ± 0.1	2.5 ± 0.1	10.6 ± 0.3	5.3 ± 0.2	5.1 ± 0.2	5.0 ± 0.1	4.9 ± 0.1
[67]Ga	4.1 ± 0.3	1.5 ± 0.1	1.5 ± 0.1	1.4 ± 0.1	1.4 ± 0.1	8.2 ± 0.3	3.1 ± 0.1	3.0 ± 0.1	2.8 ± 0.1	2.8 ± 0.1
[51]Cr	1.4 ± 0.7	0.7 ± 0.4	0.7 ± 0.4	0.7 ± 0.4	0.7 ± 0.4	2.1 ± 0.8	1.0 ± 0.4	1.0 ± 0.4	1.0 ± 0.4	1.0 ± 0.4
[203]Pb	5.9 ± 0.2	2.2 ± 0.1	2.0 ± 0.1	1.9 ± 0.1	1.8 ± 0.1	11.9 ± 0.2	4.5 ± 0.1	4.2 ± 0.1	3.9 ± 0.1	3.7 ± 0.1
[169]Yb (7)	31.1 ± 17.9	8.5 ± 4.9	7.2 ± 4.2	5.5 ± 3.2	5.3 ± 3.1	46.6 ± 20.2	12.9 ± 5.6	10.9 ± 4.7	8.3 ± 3.6	7.9 ± 3.4

* Range of doses < 0.05 rad.

TABLE 4. COMPARATIVE USEFUL PHOTON FLUX FOR SAME APPROXIMATE RADIATION DOSE TO SPINAL CORD

Compound	Quantity administered intrathecally (mCi)	Useful gamma rays		Relative useful photon flux		
		Energy (keV)	Abundance per disintegration	At 0 hr	At 24 hr	At 48 hr
^{131}I-IHSA*	0.1	364	0.83 (11)	0.4	0.4	0.3
[169]Yb-DTPA*	0.4	177 and 198	0.55 (13)	1.0	1.0	1.0
^{99m}Tc-DTPA	9.0	140	0.88 (11)	35	2.2	0.1
[113m]In-DTPA	12.0	393	0.65 (11)	35	0.002	Negligible
^{111}In-DTPA	0.9	172, 247	0.90, 0.94 (13)	3.6, 3.8	2.9, 3.0	2.3, 2.4
^{67}Ga-DTPA	1.5	91–388	0.02–0.4 (12)	0.1–2.6	0.08–2.0	0.05–1.5
[51]Cr-DTPA	3.2	320	0.09 (11)	1.3	1.3	1.3
[203]Pb-DTPA	1.2	279	0.81 (13)	4.3	3.2	2.4

* Utilizing results presented in Ref. 7.

These average values are solely caused by photons and persist throughout the cord and nerve roots. The doses from [113m]In-DTPA fall off most slowly with depth, as expected from the [113m]In electron dose reduction coefficients (Figs. 3 and 4). Technetium-99m gives the lowest radiation doses to the spinal cord and nerve roots, per millicurie of radioactive DTPA administered, followed by [113m]In and ^{51}Cr, ^{67}Ga, ^{111}In, and [203]Pb. The absorbed doses at the surface of the spinal cord and nerve roots per millicurie of tagged DTPA are greatest for [203]Pb (Table 3) but, as expected from the electron dose reduction coefficients (Figs. 3 and 4), these decrease more rapidly with depth than those for ^{111}In, which gives the largest doses per millicurie away from the surface.

The absorbed radiation dose estimates, however, do not give any indication of the relative usefulness for cisternography of each DTPA radiopharmaceutical in terms of useful photon flux and therefore image quality at various times after injection. Table 4 summarizes, for the six DTPA radionuclide tags under consideration and for [169]Yb and [131]I (7), the useful gamma rays and their abundance per disintegration. Also listed in Table 4 are the quantities of each radioactive DTPA compound and of ^{131}I-IHSA which, intrathecally administered, would result in about the same average dose to the spinal cord and about the same total radiation dose at 0.01 cm depth [the approximate pia thickness (19)]. Hence, utilizing this information and the physical decay of the radionuclides and assuming other things equal, the useful photon flux from the radiopharmaceuticals at 0, 24, and 48 hr after intrathecal administration of the quantities listed were determined (Table 4), relative to [169]Yb-DTPA. The values given for ^{131}I-IHSA at 24 and 48 hr assume that the rates of clearance of albumin and DTPA from the spinal subarachnoid space are equal. However, since the chelates appear to clear more rapidly from the cerebrospinal fluid circulation than albumin (5,6), the useful photon flux of ^{131}I-IHSA would be expected to increase with time following injection relative to the radioactive chelates, and hence the photon flux ratios of ^{131}I-IHSA compared to [169]Yb-DTPA at 24 and 48 hr will be slightly greater than given in Table 4.

Inspection of the photon flux ratios in Table 4 indicates that all the DTPA radiopharmaceuticals are superior to ^{131}I-IHSA. When useful cisternographic information can be obtained within 24 hr, ^{99m}Tc-DTPA offers considerable photon flux advantages as a cisternographic imaging agent. The longer physical half-lives (Table 1) of the radionuclides other than [113m]In and ^{99m}Tc result in photon fluxes which change much less drastically with time during the 48 hr after administration. Of the multiple-photon emissions from ^{67}Ga, the 93-keV gamma ray has the greatest abundance per disintegration: 0.4 (12). Lead-203-DTPA and ^{111}In-DTPA appear to be the best cisternographic agents of those considered. For the combined abundance (1.84) of both ^{111}In gamma rays, the photon flux from 0.9 mCi ^{111}In-DTPA is greater than that from 0.4 mCi [169]Yb-DTPA by a factor of 7.4–4.7 over a 48-hr period.

Other advantages in using radioactive chelates for cerebrospinal fluid scanning over ^{131}I-IHSA have been well documented (1–7). The choice of radionuclide tag for the chelate is based on the physical characteristics of each radionuclide and the radiation dose to spinal cord and nerve roots. Of the radionuclide-labeled chelates considered in this report, the following additional observations can be made. The higher-energy gamma rays of ^{111}In, ^{67}Ga, ^{51}Cr, and [203]Pb are not so flexible regarding collimation, while conversely

the lower-energy gamma rays of ^{169}Yb, ^{99m}Tc, ^{111}In, and ^{67}Ga are most suitable for use with the various new low-energy scintillation camera collimators commercially available. Short-lived ^{113m}In and ^{99m}Tc are not suitable for delayed studies or strict radiopharmaceutical quality control prior to administration. These disadvantages do not apply to ^{203}Pb, ^{111}In, and ^{67}Ga, with intermediate physical half-lives of 2–3 days (Table 1), or to ^{51}Cr and ^{169}Yb, with long physical half-lives, which additionally provide long radiopharmaceutical shelf-life.

ACKNOWLEDGMENT

REFERENCES

1. BELL EG, SUBRAMANIAN G, McAFEE JG, et al: Radiopharmaceuticals for cisternography. In Cisternography and Hydrocephalus, Springfield, Ill, CC Thomas, 1972, pp 161–171

2. HOSAIN F, SOM P, JAMES AE, et al: Radioactive chelates for cisternography: The basis and the choice. In Cisternography and Hydrocephalus, Springfield, Ill, CC Thomas, 1972, pp 185–193

3. HOSAIN F, SOM P: Chelated ^{111}In: An ideal radiopharmaceutical for cisternography. Br J Radiol 45: 677–679, 1972

4. SOM P, HOSAIN F, WAGNER HN, et al: Cisternography with chelated complex of ^{99m}Tc. J Nucl Med 13: 551–553, 1972

5. GOODWIN DA, SONG CH, FINSTON R, et al: Preparation, physiology, and dosimetry of ^{111}In-labeled radiopharmaceuticals for cisternography. Radiology 108: 91–98, 1973

6. HARBERT JC, REED V, McCULLOUGH DC: Compari-

son between ^{131}I-IHSA and ^{169}Yb-DTPA for cisternography. J Nucl Med 14: 765–768, 1973

7. MORIN RL, BROOKEMAN VA: ^{169}Yb-DTPA distribution and dosimetry in cisternography. J Nucl Med 15: 786–796, 1974

8. HOSAIN F, REBA RC, WAGNER HN: Measurement of glomerular filtration rate using chelated ytterbium-169. Int J Appl Radiat Isot 20: 517–521, 1969

9. SOM P, HOSAIN F, WAGNER HN: Kinetics of agents used for cisternography. J Nucl Med 12: 396, 1971

10. LOEVINGER R, BERMAN M: A schema for absorbed-dose calculations for biologically distributed radionuclides. MIRD Pamphlet No 1, J Nucl Med 9 (Suppl 1): 7–14, 1968

11. DILLMAN LT: Radionuclide decay schemes and nuclear parameters for use in radiation-dose estimation. MIRD Pamphlet No 4, J Nucl Med 10 (Suppl 2): 5–32, 1969

12. DILLMAN LT: Radionuclide decay schemes and nuclear parameters for use in radiation-dose estimation, Part 2. MIRD Pamphlet No 6, J Nucl Med 11 (Suppl 4): 5–32, 1970

13. DILLMAN LT, VON DER LAGE FC: Radionuclide Decay Schemes and Nuclear Parameters for Use in Radiation Dose Estimation, MIRD Pamphlet No 10, New York, Society of Nuclear Medicine, 1975

14. ELLETT WH, HUMES RM: Absorbed fractions for small volumes containing photon-emitting radioactivity. MIRD Pamplet No 8, J Nucl Med 12 (Suppl No 5): 25–32, 1971

15. WIDMAN JC, POWSNER ER: Energy absorption in cylinders containing an axial source. J Nucl Med 7: 407–415, 1966

16. BROOKEMAN VA, FITZGERALD LT, MORIN RL: unpublished data

17. BERGER MJ: Beta-ray dosimetry calculations with the use of point kernels. In Medical Radionuclides—Radiation Dose and Effects, Oak Ridge, USAEC, 1970, pp 63–86

18. BERGER MJ: Improved point kernels for electron and beta-ray dosimetry. Washington, NBS, NBSIR 73–107, 1973

19. HILDITCH TE: Radiation dose in isotope encephalography. Lancet 2: 573–574, 1968